JOURNAL OF GENERAL VIROLOGY

RESEARCH ARTICLE

Sharma *et al.*, *Journal of General Virology* 2017;98:1785–1794

DOI 10.1099/jgv.0.000817

Purification and characterization of adenovirus core protein VII: a histone-like protein that is critical for adenovirus core formation

Gaurav Sharma,[1] Nithesh Moria,[1] Martin Williams,[2] Bankala Krishnarjuna[2] and Colin W. Pouton[1,*]

Abstract

Adenovirus protein VII is a highly cationic core protein that forms a nucleosome-like structure in the adenovirus core by condensing DNA in combination with protein V and mu. It has been proposed that protein VII could condense DNA in a manner analogous to mammalian histones. Due to the lack of an expression and purification protocol, the interactions between protein VII and DNA are poorly understood. In this study we describe methods for the purification of biologically active recombinant protein VII using an *E. coli* expression system. We expressed a cleavable fusion of protein VII with thioredoxin and established methods for purification of this fusion protein in denatured form. We describe an efficient method for resolving the cleavage products to obtain pure protein VII using hydroxyapatite column chromatography. Mass spectroscopy data confirmed its mass and purity to be 19.4 kDa and >98 %, respectively. Purified recombinant protein VII spontaneously condensed dsDNA to form particles, as shown by dye exclusion assay, electrophoretic mobility shift assay and nuclease protection assay. Additionally, an *in vitro* bioluminescence assay revealed that protein VII can be used to enhance the transfection of mammalian cells with lipofectamine/DNA complexes. The availability of recombinant protein VII will facilitate future studies of the structure of the adenovirus core. Improved understanding of the structure and function of protein VII will be valuable in elucidating the mechanism of adenoviral DNA condensation, defining the morphology of the adenovirus core and establishing the mechanism by which adenoviral DNA enters the nucleus.

INTRODUCTION

Adenoviruses are non-enveloped, icosahedral viruses, consisting of a capsid containing approximately 36 kb double-stranded linear DNA [1, 2]. They are approximately 90 nm in diameter and are assembled from 13 different proteins, commonly categorised into three types: capsid proteins, cement proteins and core proteins [3]. The outward face of the capsid consists of three proteins; hexon, penton and fibre. Hexon is the major adenoviral capsid protein, present as 820±40 copies per virion [2]. Penton is a 63.3 kDa adenoviral capsid protein, located as pentamers at the vertexes of the adenoviral icosahedron [2]. The fibre is a 35.3 kDa protein, present as 36 copies per virion, one trimer per apex [2]. Adenoviruses contains four cement proteins, IIIa, VI, VIII and IX, that play a vital role in stabilizing the adenoviral skeletal framework by interacting with the capsid proteins [2, 3]. Cement proteins are also believed to play roles in adenoviral assembly, disassembly and endosomal escape [4].

The adenovirus core consists of three basic proteins – mu peptide, protein V and protein VII – and the non-basic terminal protein [5–7]. There are only two copies of terminal protein per adenovirus genome, each of which is covalently linked to one of the 5′ terminal ends of the dsDNA [8, 9]. Terminal protein is believed to protect the adenoviral DNA from nucleases and plays a functional role in DNA replication [10]. The function of the short polypeptide mu, which is a cleavage product derived from protein X [5], is not fully understood; however, its highly basic amino acid sequence suggests a role in assisting core proteins in tight DNA condensation. Protein V appears to form a shell around the DNA–protein VII complex, thus establishing a link between core and capsid proteins [11]. Protein V has been postulated to aid in DNA condensation, perhaps in a manner analogous to histone H1 in mammalian chromatin [12]. Protein VII is well known to be the predominant adenoviral core protein and forms the basis of the chromatin-like structure with adenoviral DNA [1, 5, 13–15]. Protein VII is a highly basic protein, with 46 % of its amino acids being positively charged.

Received 12 January 2017; Accepted 22 April 2017

Author affiliations: [1]Drug Delivery, Disposition and Dynamics, Monash Institute of Pharmaceutical Sciences (MIPS), Monash University, Melbourne, Vic, 3052, Australia; [2]Medicinal Chemistry, Monash Institute of Pharmaceutical Sciences, Monash University, Melbourne, Vic, 3052, Australia.
***Correspondence:** Colin W. Pouton, colin.pouton@monash.edu

Keywords: adenovirus protein VII; core protein; expression; purification; DNA binding.

Pulse-chase experiments demonstrated that protein VII exists as pro-VII, a precursor form of protein VII, in the immature virus [16–18]. The pro-VII is cleaved between glycine-24 and alanine-25 by an adenoviral endopeptidase (AVP) before the virus matures [19, 20]; the resultant protein VII consists of 198 amino acids, this being the relevant fragment required to understand the structure of the virus core. In common with histones, adenoviral protein VII possesses more than one nuclear localization sequence, and could have a role in translocating adenoviral DNA to the nucleus of infected mammalian cells. However, recombinant adenoviral core protein VII has not been studied in relation to its possible role in delivering adenoviral DNA, either *in vitro* or *in vivo*.

Although detailed structural information has been obtained for the adenoviral capsid proteins, the structural biology of the major adenoviral core proteins, especially protein VII, remains unclear [16]. This is due to the fact that the adenoviral core is disordered when compared to the icosahedral order within the capsid, and therefore structural information cannot be determined using the currently available methods, such as X-ray diffraction, mass-spectroscopic analysis or cryo-electron microscopy [2, 21].

With the aim of improving our knowledge of adenoviral core protein VII, we embarked on its biosynthesis using rDNA technology in bacterial expression systems. To the best of our knowledge, there are no optimized protocols for preparing and purifying protein VII using an *E. coli* expression system. Haruki *et al.* [22] reported that protein VII cannot be adequately expressed in its functional form (amino acids 25–198)22. These authors expressed pro-VII (the immature form of protein VII) first, since this apparently can be expressed robustly, before cleaving the pro-protein to give mature protein VII [22]. To achieve this, adenoviral protease itself had to be expressed and purified, making this a labour-intensive method. Although this protocol produced functional protein VII, the purity and yield obtained were not reported. Hence our desire to attempt the expression and purification of mature protein VII (25–198) in *E. coli* expression systems.

RESULTS

Expression and purification of protein VII

The thioredoxin–protein VII (Trx–VII) fusion protein was overexpressed by cultivating isopropyl β-D-1-thiogalactopyranoside (IPTG)-induced *E. coli* BL21 (DE3) cells for 6 h in super-optimal broth with catabolite repression medium (SOC). Highly soluble protein at an estimated size of 37.5 kDa was obtained at 25 °C (Fig. 1a, lanes 2–5). A considerable mass of Trx–VII was found in an insoluble fraction at 37 °C, presumably due to its packaging into inclusion bodies (Fig. 1b, lanes 7–10). The soluble fusion protein did not bind strongly to the Ni^{2+}-charged HisTrap HP column and a large fraction of soluble Trx–VII appeared in the flow-through (gel not shown). This implied that the 6×His-tag of the fusion protein was unavailable for binding to Ni^{2+}, as has been reported previously [23, 24]. To allow efficient binding of Trx–VII fusion protein to Ni^{2+} beads, in this study the purification was carried out under denaturing conditions. Surprisingly, under these conditions the Trx–VII was eluted by the imidazole gradient in several fractions, resulting in wide and poorly defined peaks (Fig. 2a, b). This could have been due to two different types of interaction taking place during the protein VII purification protocol: interaction of 6×His-tag and Ni^{2+} ions, and non-specific binding of VII to the nitrilotriacetic acid (NTA) beads. In the latter case, the highly basic nature of protein VII probably allows VII to bind to the NTA beads by displacing the Ni^{2+} ions. The non-specific binding prevented clean elution of VII at a particular concentration of imidazole.

After refolding, the fusion protein was dialysed in 20 mM Tris (pH 8) buffer and subjected to tobacco etch virus (TEV) cleavage at 34 °C for 3 h. After cleavage, three bands corresponding to TEV enzyme (27 kDa), protein VII (19.4 kDa) and Trx (17.9 kDa) were observed by SDS-PAGE (Fig. 2c). Although VII appeared at a slightly higher molecular mass than expected, its integrity was confirmed using LCMS (Fig. 4). The Trx–VII-pET32a+ construct was designed such that the 6×His-tag remained with the Trx after cleavage,

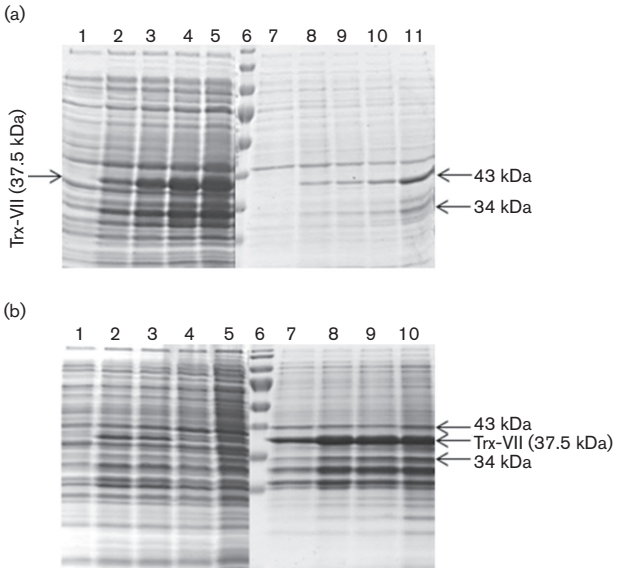

Fig. 1. SDS-PAGE analysis of protein VII expression in *E. coli* BL21 (DE3) cells. (a) Protein VII expression at 25 °C induced with 0.5 mM IPTG. Lanes 1 to 5 and 7 to 11 were loaded with soluble and insoluble fractions, respectively. Lanes 1 and 7: no IPTG. Lanes 2 and 8 : 2 h; 3 and 9 : 4 h; 4 and 10 : 6 h; 5 and 11 : 8 h induced with IPTG. (b) Expression profile at 37 °C induced with 1 mM IPTG. Lanes 1 to 5 and 7 to 10 were loaded soluble and insoluble fractions, respectively. Lane 1: no IPTG. Lanes 2 and 7 : 2 h; lanes 3 and 8 : 4 h; lanes 4 and 9 : 6 h; lanes 5 and 10 : 8 h induced with IPTG. Lane 6 in Fig. 1(a, b) is a protein marker.

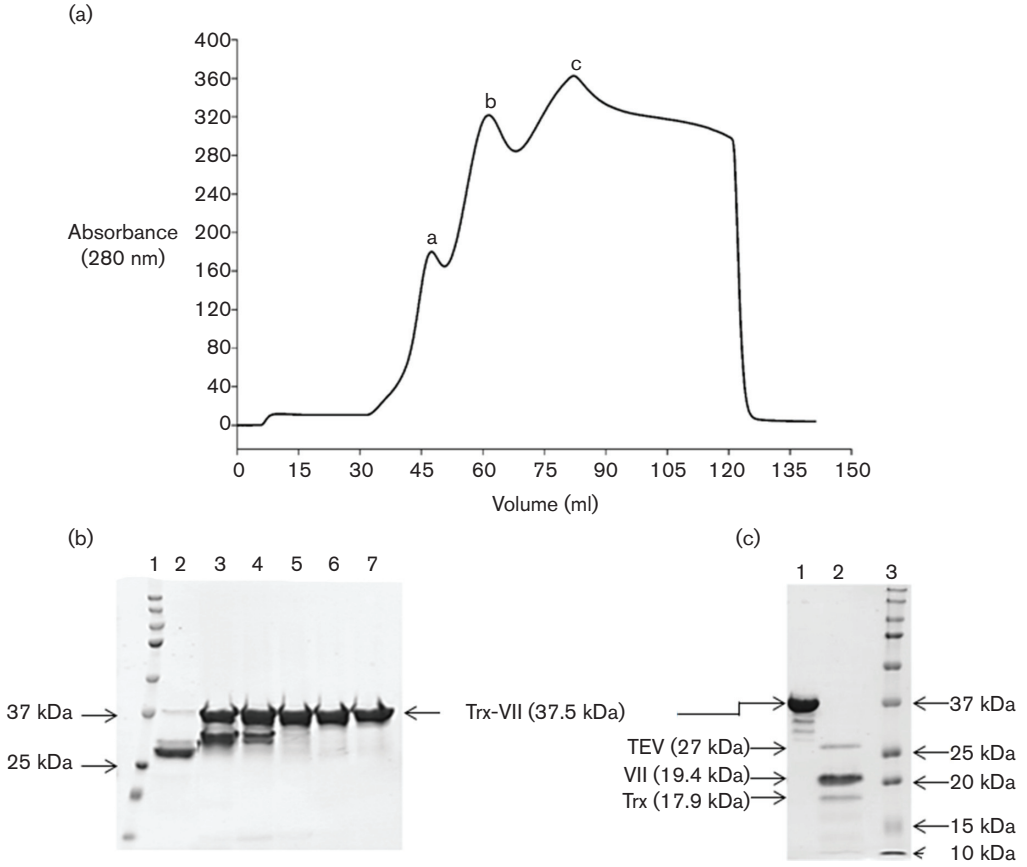

Fig. 2. Purification of Trx–VII fusion protein under denaturing conditions and TEV cleavage reaction. (a) The FPLC chromatogram displays the purification profile of Trx–VII fusion protein using a HisTrap HP affinity column. The peaks are defined in Fig. 2(b). (b) SDS-PAGE analysis of FPLC fractions. Lane 1: protein marker. Lane 2: peak a; lanes 3 and 4: peak b; and lanes 5, 6 and 7: peak c in the FPLC chromatogram. (c) SDS-PAGE analysis of the TEV cleavage reaction. Lane 1: Trx–VII fusion protein; lane 2: TEV cleavage reaction; and lane 3: protein marker.

leaving protein VII in its native form. The TEV protease used for cleavage was also tagged with 6×His-tag. This strategy was designed such that when the cleavage reaction containing all three proteins was introduced to either Ni^{2+} beads or the HisTrap HP affinity column, Trx and TEV would bind to the Ni^{2+} whereas VII would elute with the void volume. This strategy surprisingly was not successful. Protein VII eluted with Trx and TEV after imidazole elution, which was either the result of its highly cationic nature, non-specific binding to the NTA beads or binding to the other two proteins (data not shown). Among several chromatographic techniques attempted, hydroxyapatite column chromatography produced the best separation of the three proteins, allowing isolation of pure recombinant protein VII (Fig. 3).

The mass and purity of the protein VII as evaluated by LC-MS were 19.4 kDa and 98.7 %, respectively (Fig. 4). A Western blot confirmed the correct identity of VII when stained with anti-adenoviral type-5 sera (Fig. 5b). The VII in solution was stable at various temperatures for 24 h, as determined by SDS-PAGE (Fig. 5).

Protein VII possesses DNA-condensing activity and can enhance transfection

The ability of VII to condense DNA was evaluated by an electrophoretic mobility shift assay (EMSA) and a dye exclusion assay (DEA). As VII was added to DNA, in proportions defined by the charge ratio (+/−), the migration of the VII–DNA complex was retarded on an agarose gel (Fig. 6a). DNA alone (negative control) migrated at the normal rate into the agarose gel as expected (Fig. 6a, lane 1). Protein VII caused complete retention of the DNA at the origin at charge ratios of 2 or above. In a nuclease protection assay (NPA), VII provided complete DNA protection against DNase-I treatment at a charge ratio of 3 (Fig. 6b, lane 6). These data confirm the strong complexation of protein VII and DNA. At a charge ratio of 2, partial stability of the complex was observed; however, between charge ratios 0 and 2 the complexes formed were unstable and were completely digested by nuclease (Fig. 6b). When investigated using the DEA, protein VII condensation reduced access of SYBR gold dye to the DNA by 93 %. No further increase in dye exclusion was observed at (+/−) charge

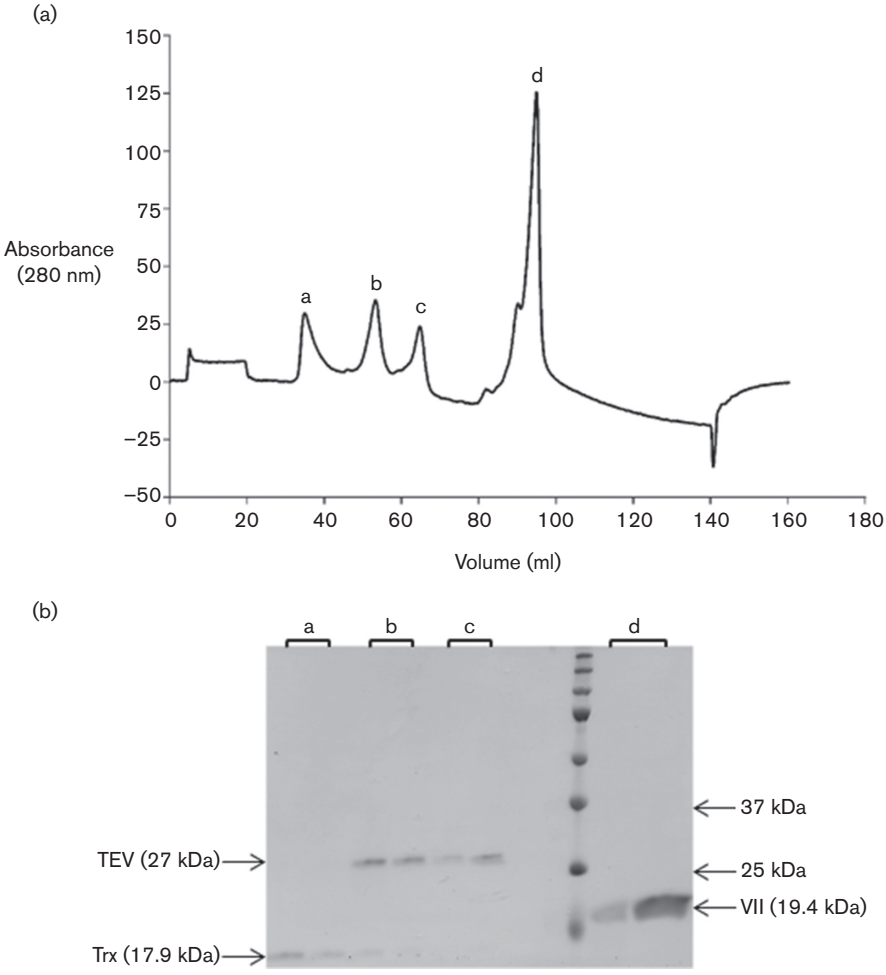

Fig. 3. Protein VII purification using hydroxyapatite column chromatography. (a) The FPLC chromatogram showing the purification profile of VII. Peak a: Trx protein; peaks b and c: TEV enzyme; and peak d: protein VII. (b) SDS-PAGE analysis of the fractions shown in Fig. 3(a). Lane 8: protein marker.

ratios greater than 2 (Fig. 6c). The DEA results are in agreement with EMSA and NPA, and validate the ability of protein VII to form tight complexes with double-stranded DNA.

Having demonstrated that protein VII condensed DNA, we investigated whether it could be used as part of a transfection complex which includes lipofectamine (LF). We found that 1 µl LF partially condensed 1 µg DNA, so that the particles formed were not prone to aggregate in OptiMEM. This resulted in low transfection efficiency (Fig. 7). In contrast, 2 µl LF fully condensed 1 µg DNA to form cationic particles and resulted in a >2000-fold increase in the transfection efficiency when compared to 1 µl LF. Therefore, particles formed by 2 µl LF were used as a positive control. To provide an appropriate comparison with respect to the positive control, 3.1 µg protein VII was added to 1 µl LF to produce a charge ratio equivalent to that of the positive control. *In vitro* transfection of MDA-MB-231 breast cancer cells was significantly enhanced in the presence of protein VII (Fig. 7).

DISCUSSION

The high proportion of positively charged amino acid residues, particularly arginine, gives protein VII histone-like DNA binding properties. However, unlike VII, histones mainly acquire their net positive charge from lysine rather than arginine residues. Interestingly, both histones and VII contain alanine-rich regions [25], even though the predominant basic amino acid composition is different.

A mutant adenovirus, HAdV-C2_TS-1 (TS-1), containing a single-point mutation in the AVP sequence, is assembled with pro-VII rather than the trimmed protein found in the wild-type virion. Interestingly, TS-1 is more stable and more compact than the wild-type virion but has reduced infectivity [16, 26, 27]. Besides protein VII, in TS-1 several other virion-associated proteins are in unprocessed forms, which results in structural changes in the virion that affect its function. The internal pressure in TS-1 has been reported to be lower and the capsid wall is softer than in the wild-type virion [28]. In terms of function, TS-1 has reduced ability to escape from

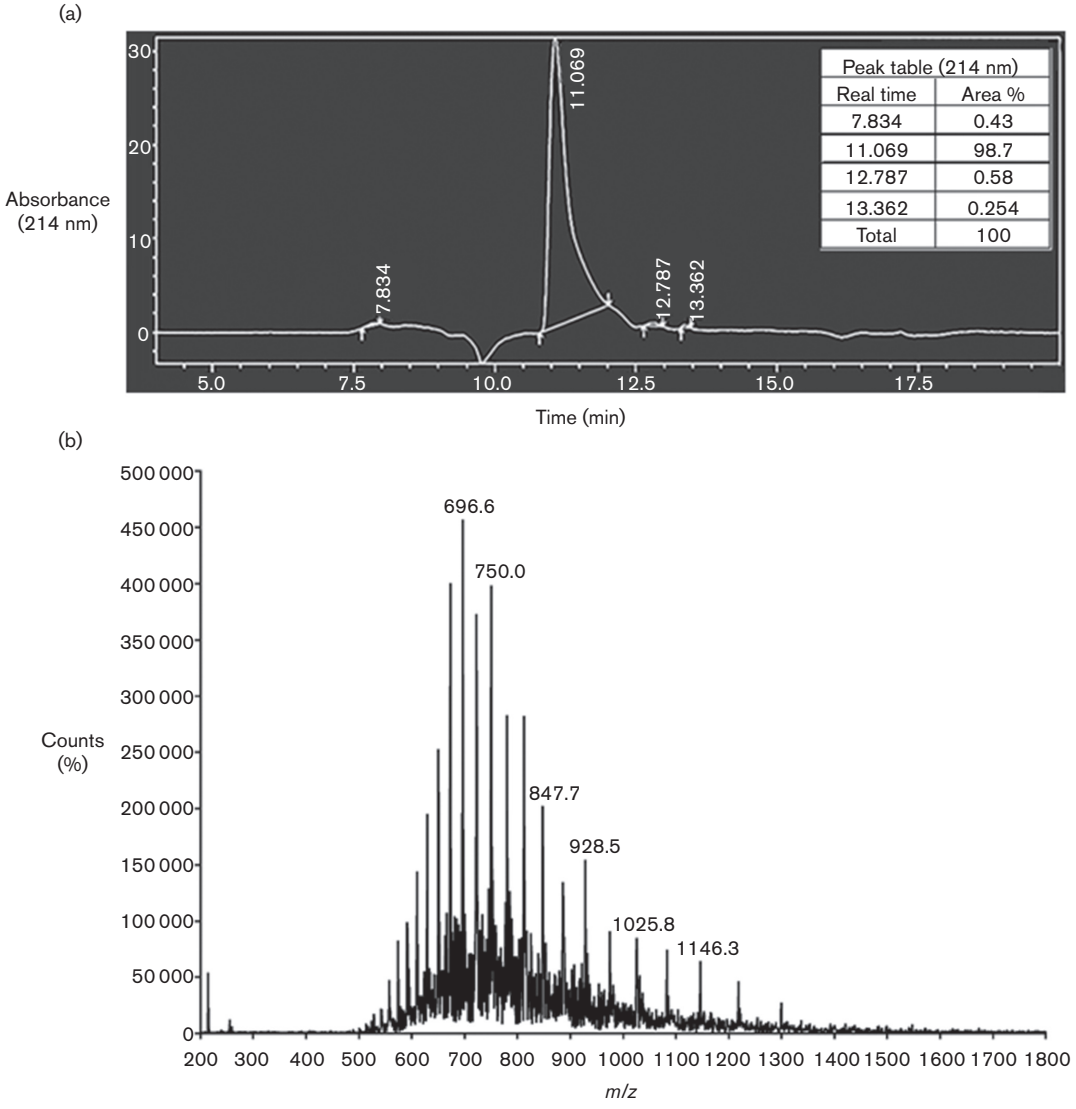

Fig. 4. LC-MS chromatogram of purified protein VII at 214 nm. (a) The peak eluted at around 11 min represents recombinant protein VII. The table at the top right shows the purity levels of VII. The purity of VII was 98.7 %. (b) Charge state distribution (*m*/*z*) of protein VII.

endosomes to the cytoplasm, and thus has reduced opportunity to deliver its DNA to the nucleus. This malfunction may be linked to the compact core and lower internal pressure in TS-1 preventing the uncoating of the capsid in response to host cell cues [29]. The significance of the physico-mechanical properties of virions for the consequences of their interaction with host cells has been discussed by Greber [30]. In the case of adenoviruses, protein VI molecules are required to dissociate and interact with the plasma or endosomal membrane [31] prior to escape of the virion from the endosome. Given that protein VII is the major core protein, its trimming from pro-VII is likely to be a significant factor in the pressurization of the mature virion.

Precise functional and structural details concerningis predominately due to the unavailability of recombinant proteins VII and V. The working protocol for the purification of VII generated during the present study will partly overcome this problem, although it does not allow the fully condensed core to be assembled without protein V.

The successful approach we used was to purify protein VII in fusion with thioredoxin protein, although the cationic nature of protein VII still presented challenges during cleavage and purification. The Trx–VII fusion product expressed optimally at 25 °C in soluble fractions in the various BL21 strains tested. Unfortunately, the fusion protein did not bind to either Ni^{2+} beads or a HisTrap HP affinity column. This was presumably due to the occlusion of the 6×His-tag within the folded conformation of VII. This finding was in agreement with other studies, where a 6×His-tag coupled to protein VII was not accessible for binding to nickel [24]. In

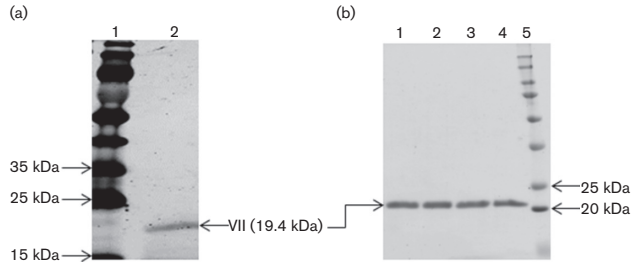

Fig. 5. (a) Western blot analysis of protein VII using anti-adenoviral type-5 antibody. Lane 1: protein VII. Lane 2: protein marker. (b) Thermal stability evaluation of recombinant protein VII. Lane 1: protein marker. Lanes 2, 3, 4 and 5 represent the stability of protein VII at different temperatures: RT, 4, −20 and −80 °C, respectively, incubated for 24 h.

our study Trx–VII was denatured with 6M Gdn-HCl before loading onto the HisTrap HP affinity column. Although the Trx–VII fusion protein was achieved with high purity, it eluted in larger volumes and with a broader peak than expected. This behaviour of the fusion protein was likely due to the highly cationic nature of VII. Nevertheless, we were successful in purifying a milligram of the fusion protein with high purity from each litre of culture, due to the high expression levels achieved with this construct.

The Trx–VII construct was designed with the aim that upon TEV cleavage, the 6×His-tag would remain coupled to Trx and VII would lack a 6×His-tag. The TEV enzyme used for cleavage reaction possessed its own 6×His-tag for ensuring its binding to nickel upon cleavage. Thus, when cleaved material was passed through the nickel affinity chromatography, VII should have eluted in the flow-through fraction, whereas 6×His-tagged Trx and TEV enzyme were expected to bind to the beads and elute at a higher concentration of imidazole. TEV protease efficiently cleaved the fusion protein and three bands representing Trx, TEV and protein VII were observed by SDS-PAGE (Fig. 2c). However, unexpectedly, after TEV cleavage it became extremely challenging to isolate VII using Ni^{2+} and Co^{2+} immobilized-metal affinity chromatography (IMAC). VII bound non-specifically to TEV and Trx, which prevented the proteins from being eluted at their usual elution time. All three proteins were

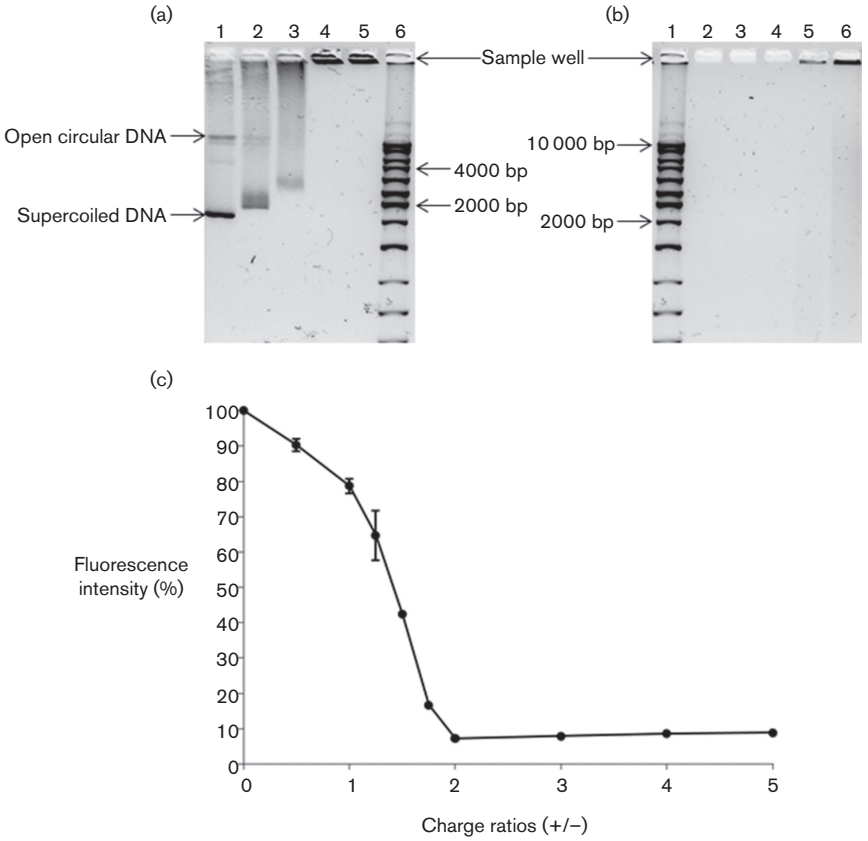

Fig. 6. DNA binding analysis of recombinant VII. (a) EMSA at increasing charge ratios of VII. Lane 1: pDNA. Lanes 2, 3, 4 and 5 represent pDNA and protein VII complexes at charge ratios of 0.5, 1, 2 and 3, respectively. Lane 6 : 1 kb DNA ladder. (b) Nuclease protection assay on pDNA–VII complex. Lane 1 : 1 kb DNA ladder; lane 2: DNA; lanes 3–6: pDNA-VII complex at charge ratios of 0.5, 1, 2 and 3, respectively. (c) Condensation profile of pDNA–VII complexes in the DEA. Protein VII at increasing charge ratios was incubated with the same concentration of pDNA for 30 min before SYBR gold dye was added to each reaction and the fluorescence was measured.

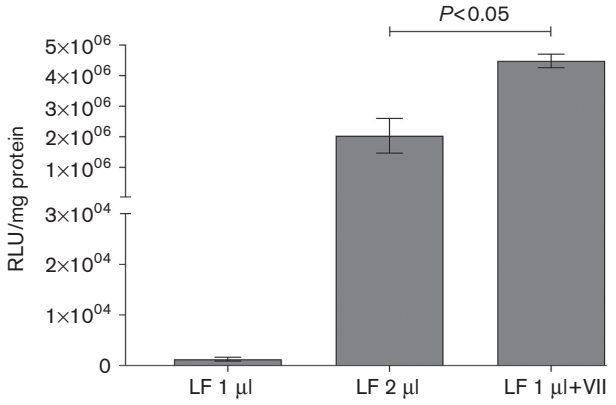

Fig. 7. Transfection of MDA-MB-231 cells by lipoplexes or LPD particles. 1 µg DNA was administered to each well complexed with either 1 or 2 µl lipofectamine (lipoplexes), or alternatively with LPD particles produced by complexing 1 µg DNA with 1 µl lipofectamine and 3.1 µg protein VII. The LPD particles were adjusted to a charge ratio (+/−) that was equivalent to that of the 2 µl lipoplexes. Twenty-four hours after transfection the bioluminescence was measured by the Nano-Glo luciferase assay system (Promega). A two-tailed unpaired *t*-test was used to justify the significance level and the data are represented as mean±SEM (*n*=3 biological replicates).

found in both the eluted and flow-through fractions when purified with Ni^{2+} beads in separate purifications. This was most likely due to the highly basic nature of VII, which allowed it to bind non-specifically with Trx and TEV.

Purification of VII from the other two proteins proved to be extremely challenging. The protein remained on the resin even after the beads were washed with 1 M imidazole. The Ni^{2+} and protein VII interaction was initially thought to be non-specific; however, this interaction was surprisingly strong and may have been the result of high affinity for the metal ions. Interestingly, Zoroddu *et al.* 32] reported that the histidine located at the 18th position of the N-terminal tail region of histone H4 forms a stable coordination bond with Ni^{2+}. This metal binding site for Ni^{2+} comes from donor atom-like nitrogen of the imidazole ring of histidine [33]. As a result of this interaction, a conformational change in the structure of histone H4 was reported [34]. This change to the structure of histone dramatically increased the α-helical content of the histone [35], thereby affecting the acetylation, methylation and ubiquitylation process of DNA [36–38]. This suggests that protein VII, being similar to histones in its DNA-binding properties, may also have formed stable coordination bonds between the histidine residues in protein VII and the Ni^{2+} on the resin. Our conclusion was that recombinant protein VII could not be purified efficiently using nickel-affinity chromatography.

To separate VII from Trx and TEV, several chromatographic techniques, including hydrophobic-interaction chromatography, cation-exchange chromatography, heparin chromatography, hydroxyapatite-column chromatography and reverse-phase HPLC, were explored. Protein VII was successfully purified with optimal purity using hydroxyapatite-column chromatography. This stationary phase separated Trx, TEV and protein VII at different elution times based on their isoelectric point. It is worth noting that the pI values of Trx, TEV and VII are 5.48, 8.8 and 12.34, respectively. The purity thus obtained was >99 and 98.7 % when measured with densitometry using Image J software (not shown) and liquid chromatography-mass spectroscopy (LC-MS), respectively. The pure recombinant VII was stable for at least 3 days at four different temperatures (Fig. 5a).

Protein VII condensed plasmid DNA to form particulate complexes which reduced the access of SYBR gold by 93 % in a DEA, completely restricted the mobility of the plasmid DNA into an agarose gel at (+/−) charge ratios above 3, and protected DNA from exonuclease activity. These assays are consistent with the expectation that protein VII is the main DNA-condensing protein in the adenovirus core. Through electron microscopy, Newcomb *et al.* [39] suggested that the core of the adenovirus exists in the form of nucleosome-like structures called adenosomes. It has been estimated that approximately 180 such adenosomes condense the DNA in the adenoviral core. These authors also suggested that one adenosome consists of six copies of VII, one copy of V and 150 to 200 base pairs of DNA, in agreement with the results of Corden *et al.* in 1976 [40]. Other groups also confirmed the nucleosome-like structure of the protein VII and DNA complex through electron microscope studies [1, 7, 41, 42, 43]. The stoichiometry and structure of the core remains to be established. Recent studies indicated that there are 148 ±15 copies of protein V and 527±44 copies of protein VII per virion [2]. Oostrum and Burnett estimated in earlier studies that there are approximately 800 copies of protein VII present per virion43. A prevailing model of the core suggests that there are approximately 180 nucleosome-like units, each made up of three subunits of dimeric protein VII and one copy of protein V [12]. This model predicts 1080 copies of protein VII, per virion which is far in excess of the 527±44 copies extracted by Heck and colleagues [2]. The ratio of six copies of protein VII to one of protein V is also brought into question by the latter studies, which extracted approximately 3.5 copies of protein VII for each copy of protein V. Whilst our studies indicate that protein VII has strong DNA-condensing properties, it will be necessary to obtain recombinant protein V to explore whether nucleosomes can be produced *in vitro* that can model the adenovirus core. At this stage it is possible to explore the value of introducing protein VII into lipoplexes to produce lipid/protein/DNA (LPD) complexes. Such complexes have the potential to form more organized transfection systems than lipid/DNA complexes. Complexation of DNA with pVII alone was ineffective, as expected, because such complexes have no mechanism for endosomal escape. LPD complexes containing both protein VII and LF performed more efficiently than particles formed with LF alone, which is consistent with the hypothesis that they formed more condensed particles for transfection (Fig. 7).

In summary, we have identified a working protocol for the expression and purification of protein VII, as it appears in the mature virion. The purified VII was >98 % pure and functioned as a strong DNA-condensing protein, as confirmed by DEA, EMSA and NPA *in vitro*. Functional assays confirmed the DNA-binding role of VII and indicated the need to conduct experiments that compare its ability with that of other DNA-binding biomolecules such as histones, protamine, poly-L-lysine and polyethylenimine, which are used extensively in gene delivery research. Protein VII clearly has the potential to make a stable complex with circular DNA, displaying one of the necessary requirements for the construction of a non-viral gene delivery vehicle.

METHODS

Cloning a mature protein VII gene into the pET32a+ *E. coli* expression vector

To design an N-terminal Trx-6xHis-TEV-protein VII construct (Fig. 8), the mature protein VII DNA (525 bp) was PCR-amplified with Phusion High-fidelity PCR Master Mix (#F-531S, Thermo Scientific), using pAdEasy-1 plasmid (Agilent Technologies) as a PCR template. To generate amplicons with a TEV sequence-specific cysteine protease cleavage site located upstream to the protein VII, 5′-CATG CCA TGG AAA ATT TAT ATT TTC AAG GTG CCA AGA AGC GCT CCG AC-3′, forward, and 5′-GATC GGA TCC CTA GTT GCG CGG GGG GCG G-3′, reverse, primers were designed. Prior to cloning, the insert and the pET32a+ vector were digested with the restriction enzymes, Nco1 and BamH1, at 37 °C for 16 h and 6 h respectively. The digested products were then run onto a 1 % agarose gel followed by the gel extraction protocol to achieve optimal purity of the desired DNA products. Protein VII DNA and pET32a+ vector were ligated at a ratio of 3.5 : 1 using a Quick-ligation kit (M2200S, New England BioLabs) and the ligated mixture was transformed into One Shot Mach1 T1R chemically competent *E.coli* DH5α cells. Having obtained these, the colonies were screened for the correct insert by restriction digestion and the positive clones were confirmed by DNA sequencing.

Overexpression of protein VII and its extraction from *E. coli*

For protein expression, the VII-pET32a+ plasmid was transformed into *E . coli* BL21 (DE3) cells. A single colony was inoculated overnight at 250 r.p.m. in a baffled flask containing 25 ml LB medium and 50 μg ml^{-1} carbenicillin. After 16 h incubation at 37 °C, 20 ml overnight culture was added to 980 ml SOC media (2 % tryptone, 0.5 % yeast extract, 20 mM $C_6H_{12}O_6$, 10 mM NaCl, 2.5 mM KCl, 10 mM $MgCl_2$ and 10 mM $MgSO_4$, pH 7.0) containing 50 μg ml^{-1} carbenicillin, 1X trace metal mix (Teknova, California, USA) and 0.1X BME vitamin mix (Sigma). The culture was propagated until an OD_{600} of 0.6 was reached, and IPTG (0.25–1 mM) was added to induce the expression of the target protein. Cells were harvested after 6 h by centrifugation at 6000 ***g*** for 15 min in a Beckman Avanti centrifuge (Beckman Coulter, Brea, USA). The pellet was either lysed for immediate purification or stored at −80 °C for later purification. To extract protein VII, the bacterial cells were resuspended in BugBuster lysis buffer (Merck Millipore) (3 ml/1 g cell pellet) and an EDTA-free protease inhibitor tablet (Roche) was added to prevent proteolysis. The cell lysate was treated with DNase prepared in 5 mM $MgCl_2$ at a final concentration of 50 μg ml^{-1} to clear the cellular DNA. The suspension was then incubated at 25 °C for 25 min on a shaker rotating at 80 r.p.m. To ensure complete cell lysis, the suspension was sonicated four times for 20 s, each time at an output of 12w, with 30 s of cooling on ice between each sonication. The cell lysate was then centrifuged at 8000 ***g*** for 30 min at 4 °C using a JA-25.5 rotor (Beckman Avanti centrifuge). In the case of the soluble fraction, the supernatant was filtered through a 0.2 μm filter before being loaded onto the affinity column. When the protein was found in the insoluble fraction, the protein VII was purified using a standard protocol for purification from inclusion bodies.

Protein VII purification

A HisTrap HP 5 ml Ni^{2+} affinity column (GE Healthcare) was connected to a fast protein liquid chromatography (FPLC) instrument (AKTA Scientific) to purify the 6×His tagged protein. The sample was loaded at a flow rate of 1 ml min^{-1}; however, the washing (20 mM Tris, 500 mM NaCl, 20 mM imidazole, pH 8) and elution (20 mM Tris, 500 mM NaCl, 1 M imidazole, pH 8) were performed at a flow rate of 4 ml min^{-1}. A linear gradient of 0–1 M imidazole was used to elute the protein.

pET32a+-derived Trx–protein VII fusion protein was purified under denaturing conditions (6 M Gdn-HCl, 20 mM Tris, 500 mM NaCl, 10 mM imidazole, pH 8). To renature the fusion protein, on-column refolding was performed using a HisTrap HP column. Briefly, a renaturing buffer A (20 mM Tris, 500 mM NaCl; pH 8.0) was applied to the column-bound denatured protein before a gradient of 10 column volumes between buffer A and buffer B (20 mM Tris, 500 mM NaCl, 1

Fig. 8. Schematic representation of the VII-pET32a+ expression cassette. The Trx and the 6xHis tag are part of the pET32a+ vector, whereas the TEV cleavage site was added upstream to protein VII via forward primer.

M imidazole, pH 8.0) was passed through the column. The protein was dialysed using 3.5 kDa Spectra/Por 7 dialysis tubing (Spectrum Labs, USA) overnight at 4 °C in a 50 mM Tris pH 8 buffer to remove imidazole before the TEV cleavage reaction was performed (note that protein precipitation was observed when a desalting column was used to remove imidazole). On the following day, the same dialysis bag was put into a fresh 5 L volume of the same buffer for 6 h for the complete removal of imidazole. The sample was filtered through a 0.2 µm filter and the TEV cleavage was performed. In-house-expressed and purified TEV enzyme was added to the protein at a molar ratio of 1 : 100 and the reaction was incubated at 34 °C for 3 h. TCEP at 1 mM concentration was included in the reaction to enhance the efficiency of the TEV enzyme. The cleaved reaction mixture was then applied to a Bio-Scale CHT5-I ceramic hydroxyapatite, type-I column (Bio-Rad) and a linear gradient between the binding (10 mm Na_2HPO_4, pH 6.8) and elution (500 mm Na_2HPO_4, pH 6.8) buffers was used to elute the protein. The flow rate and the maximum column pressure limit were 3 ml min^{-1} and 2 MPa, respectively. The pure protein VII obtained was buffer-exchanged and concentrated in 15 mM HEPES, pH 7.4, using a Millipore concentrator.

Western blot detection of protein VII

Western blotting was performed using Bio-Rad's Trans-Blot Semi Dry system. Before transfer, the gel, the nitrocellulose membrane and the filter papers were soaked in the transfer buffer (1.44 % glycine, 0.3 % Tris and 10 % CH_3OH, pH 8.3) for 30 min. The assembly was then prepared as per the manufacturer's instructions, and the bubbles were rolled out using a tube, before transfer at 12 V for 40 min. Following transfer, the membrane was soaked in PBS for 5 min and then incubated in Odyssey blocking buffer for 1 h at room temperature. We then applied 1 : 1000 diluted rabbit *anti*-adenoviral type-5 primary polyclonal antibody (ab6892, Abcam) in blocking buffer + 0.1 % Tween 20 to the membrane. After 12 h of incubation at 4 °C, the membrane was washed four times for 5 min with PBS+0.1 % Tween 20 at room temperature. Donkey anti-rabbit secondary antibody IRD-680W, prepared as 1 in 10 000 PBS+0.1 % Tween 20, was applied to the membrane and the blot was incubated for 1 h at room temperature. The membrane was then washed four times for 5 min with PBS+0.1 % Tween 20 before the membrane was rinsed in PBS (137 mM NaCl, 2.7 mM KCl, 10 mM Na_2HPO_4 and 1.8 mM KH_2PO_4; pH 7.4). The membrane was read using an Odyssey infrared blot reader (LI-COR Biosciences).

Determination of the purity and mass of protein VII by LC-MS

The purity and mass of VII were confirmed by LC-MS. The protein was loaded onto a Jupiter C4 300A HPLC column (size=50×2.0 mM; Phenomenex, Australia) and the protein was eluted with an acetonitrile gradient between buffer A (0.1 % formic acid in Mill-Q H_2O) and buffer B (0.1 % formic acid in acetonitrile).

Protein VII–DNA binding analysis

The affinity of VII to dsDNA at different charge ratios was evaluated by an EMSA. Briefly, 5 µg ml^{-1} of pDNA (pNL1.1.CMV plasmid dsDNA; Promega, Australia) was mixed with VII atin creasing charge ratios ranging from 0 to 3 (0–0.6 µg/lane). The DNA–protein VII complex thus formed was incubated for 30 min at room temperature and analysed by 1 % agarose gel. Retardation in the migration of DNA at a particular charge ratio reflected the DNA-binding capacity of VII.

DNA-condensing potential of protein VII

The ability of VII to condense DNA was assessed using a DEA. pDNA at a concentration of 5 µg ml^{-1} was mixed with varying charge ratios (0, 0.5, 1, 1.25, 1.5, 1.75, 2, 3, 4 and 5) of VII, and incubated at room temperature for 25 min for complex formation. This was followed by the addition of SYBR gold dye with a further incubation time of 15 min. The fluorophore was excited at 492 nm and the emission wavelength was recorded at 540 nm. The fluorescence assay was performed in Corning 96-well black plates and each plate was read on an Envision plate reader (Perkin-Elmer).

Determination of the stability of condensed complexes

The ability of the cationic protein VII to protect the pDNA from being degraded upon nuclease addition was tested using a nuclease protection assay. pDNA (5 µg ml^{-1}) was complexed with increasing charge ratios (0, 0.5, 1, 2 and 3) of protein VII and complex formation was allowed for 25 min at room temperature. 10 µg ml^{-1} DNAse-I and 1 mM $MgCl_2$ was added to the complex formed and the reaction was incubated for 30 min at 37 °C. The products were run on a 1 % agarose gel to check the effect of DNAse-I on the stability of the complexes.

In vitro gene delivery using protein VII

To evaluate the ability of protein VII to enhance the transfection of mammalian cells by lipoplexes, we formed complexes with the reporter plasmid pNL1.1.CMV (Promega), which drives expression of nanoluciferase in mammalian cells. We transfected MDA-MB-231 human breast cancer cells with either lipoplexes formed with DNA and LF or LPD complexes formed by LF and protein VII. Lipoplexes were formed using 1 or 2 µl LF. LPD particles were formed using 1 µl LF and 2 µg protein VII to produce particles with a charge ratio equivalent to the 2 µl LF lipoplexes. NanoLuc nanoluciferase expression was determined after 24 h using the Nano-Glo luciferase assay system (Promega).

Funding information
The authors received no specific grant from any funding agency.

Acknowledgement
This project was supported by the award of a Monash University PhD Scholarship to G. S.

Conflicts of interest
The authors declare that there are no conflicts of interest.

Ethical statement
The work described was approved by the Monash University Biological Safety Committee and the Australian Office of Gene Technology Research.

References

1. Pérez-Berná AJ, Marion S, Chichón FJ, Fernández JJ, Winkler DC *et al.* Distribution of DNA-condensing protein complexes in the adenovirus core. *Nucleic Acids Res* 2015;43:4274–4283.
2. Benevento M, Di Palma S, Snijder J, Moyer CL, Reddy VS *et al.* Adenovirus composition, proteolysis, and disassembly studied by in-depth qualitative and quantitative proteomics. *J Biol Chem* 2014;289:11421–11430.
3. Wiethoff CM, Nemerow GR. Adenovirus membrane penetration: tickling the tail of a sleeping dragon. *Virology* 2015;479-480:591–599.
4. Reddy VS, Nemerow GR. Structures and organization of adenovirus cement proteins provide insights into the role of capsid maturation in virus entry and infection. *Proc Natl Acad Sci USA* 2014; 111:11715–11720.
5. Russell WC. Adenoviruses: update on structure and function. *J Gen Virol* 2009;90:1–20.
6. Condezo GN, Marabini R, Ayora S, Carazo JM, Alba R *et al.* Structures of adenovirus incomplete particles clarify capsid architecture and show maturation changes of packaging protein L1 52/55k. *J Virol* 2015;89:9653–9664.
7. Vayda ME, Rogers AE, Flint SJ. The structure of nucleoprotein cores released from adenovirions. *Nucleic Acids Res* 1983;11:441–460.
8. Stillman BW, Bellett AJ. An adenovirus protein associated with the ends of replicating DNA molecules. *Virology* 1979;93:69–79.
9. Rekosh DM, Russell WC, Bellet AJ, Robinson AJ. Identification of a protein linked to the ends of adenovirus DNA. *Cell* 1977;11:283–295.
10. Pronk R, Stuiver MH, van der Vliet PC. Adenovirus DNA replication: the function of the covalently bound terminal protein. *Chromosoma* 1992;102:S39–S45.
11. Liu H, Jin L, Koh SB, Atanasov I, Schein S *et al.* Atomic structure of human adenovirus by cryo-EM reveals interactions among protein networks. *Science* 2010;329:1038–1043.
12. Puntener D, Engelke MF, Ruzsics Z, Strunze S, Wilhelm C *et al.* Stepwise loss of fluorescent core protein V from human adenovirus during entry into cells. *J Virol* 2011;85:481–496.
13. Gyurcsik B, Haruki H, Takahashi T, Mihara H, Nagata K. Binding modes of the precursor of adenovirus major core protein VII to DNA and template activating factor I: implication for the mechanism of remodeling of the adenovirus chromatin. *Biochemistry* 2006;45:303–313.
14. Chen J, Morral N, Engel DA. Transcription releases protein VII from adenovirus chromatin. *Virology* 2007;369:411–422.
15. Giberson AN, Davidson AR, Parks RJ. Chromatin structure of adenovirus DNA throughout infection. *Nucleic Acids Res* 2012;40: 2369–2376.
16. Mangel WF, San Martín C. Structure, function and dynamics in adenovirus maturation. *Viruses* 2014;6:4536–4570.
17. Edvardsson B, Everitt E, Jörnvall H, Prage L, Philipson L. Intermediates in adenovirus assembly. *J Virol* 1976;19:533–547.
18. Ishibashi M, Maizel JV Jr. The polypeptides of adenovirus. V. Young virions, structural intermediate between top components and aged virions. *Virology* 1974;57:409–424.
19. Sung MT, Cao TM, Lischwe MA, Coleman RT. Molecular processing of adenovirus proteins. *J Biol Chem* 1983;258:8266–8272.
20. San Martín C. Latest insights on adenovirus structure and assembly. *Viruses* 2012;4:847–877.
21. Pérez-Vargas J, Vaughan RC, Houser C, Hastie KM, Kao CC *et al.* Isolation and characterization of the DNA and protein binding activities of adenovirus core protein V. *J Virol* 2014;88:9287–9296.
22. Haruki H, Gyurcsik B, Okuwaki M, Nagata K. Ternary complex formation between DNA-adenovirus core protein VII and TAF-Iβ/SET, an acidic molecular chaperone. *FEBS Lett* 2003;555:521–527.
23. Schmitt J, Hess H, Stunnenberg HG. Affinity purification of histidine-tagged proteins. *Mol Biol Rep* 1993;18:223–230.
24. Bornhorst JA, Falke JJ. Purification of proteins using polyhistidine affinity tags. *Methods Enzymol* 2000;326:245–254.
25. Brown DT, Westphal M, Burlingham BT, Winterhoff U, Doerfler W. Structure and composition of the adenovirus type 2 core. *J Virol* 1975;16:366–387.
26. Rancourt C, Keyvani-Amineh H, Sircar S, Labrecque P, Weber JM. Proline 137 is critical for adenovirus protease encapsidation and activation but not enzyme activity. *Virology* 1995;209:167–173.
27. Weber J. Genetic analysis of adenovirus type 2 III. Temperature sensitivity of processing viral proteins. *J Virol* 1976;17:462–471.
28. Ortega-Esteban A, Condezo GN, Pérez-Berná AJ, Chillón M, Flint SJ *et al.* Mechanics of viral chromatin reveals the pressurization of human adenovirus. *ACS Nano* 2015;9:10826–10833.
29. Snijder J, Reddy VS, May ER, Roos WH, Nemerow GR *et al.* Integrin and defensin modulate the mechanical properties of adenovirus. *J Virol* 2013;87:2756–2766.
30. Greber UF. Virus and host mechanics support membrane penetration and cell entry. *J Virol* 2016;90:3802–3805.
31. Ortega-Esteban A, Bodensiek K, San Martín C, Suomalainen M, Greber UF *et al.* Fluorescence tracking of genome release during mechanical unpacking of single viruses. *ACS Nano* 2015;9:10571–10579.
32. Zoroddu MA, Kowalik-Jankowska T, Kozlowski H, Molinari H, Salnikow K *et al.* Interaction of Ni(II) and Cu(II) with a metal binding sequence of histone H4: AKRHRK, a model of the H4 tail. *Biochim Biophys Acta* 2000;1475:163–168.
33. Halcrow MA, Christou G. Biomimetic chemistry of nickel. *Chem Rev* 1994;94:2421–2481.
34. Zoroddu MA, Peana M, Medici S, Casella L, Monzani E *et al.* Nickel binding to histone H4. *Dalton Trans* 2010;39:787–793.
35. Wang X, Moore SC, Laszckzak M, Ausió J. Acetylation increases the α-helical content of the histone tails of the nucleosome. *J Biol Chem* 2000;275:35013–35020.
36. Lee YW, Klein CB, Kargacin B, Salnikow K, Kitahara J *et al.* Carcinogenic nickel silences gene expression by chromatin condensation and DNA methylation: a new model for epigenetic carcinogens. *Mol Cell Biol* 1995;15:2547–2557.
37. Yan Y, Kluz T, Zhang P, Chen HB, Costa M. Analysis of specific lysine histone H3 and H4 acetylation and methylation status in clones of cells with a gene silenced by nickel exposure. *Toxicol Appl Pharmacol* 2003;190:272–277.
38. Nakao M. Epigenetics:interaction of DNA methylation and chromatin. *Gene* 2001;278:25–31.
39. Newcomb WW, Boring JW, Brown JC. Ion etching of human adenovirus 2: structure of the core. *J Virol* 1984;51:52–56.
40. Corden J, Engelking HM, Pearson GD. Chromatin-like organization of the adenovirus chromosome. *Proc Natl Acad Sci USA* 1976;73: 401–404.
41. Fedor MJ, Daniell E. Ionic and nonionic interactions in adenoviral nucleoprotein complexes. *J Virol* 1983;47:370–375.
42. Mirza MA, Weber J. Structure of adenovirus chromatin. *Biochim Biophys Acta* 1982;696:76–86.
43. van Oostrum J, Burnett RM. Molecular composition of the adenovirus type 2 virion. *J Virol* 1985;56:439–448.